HHS Public Access

Author manuscript

Biochim Biophys Acta Mol Basis Dis. Author manuscript; available in PMC 2022 December 01.

Published in final edited form as:

Biochim Biophys Acta Mol Basis Dis. 2021 December 01; 1867(12): 166249. doi:10.1016/j.bbadis.2021.166249.

SIRT6 controls hepatic lipogenesis by suppressing LXR, ChREBP, and SREBP1

Chaoyu Zhu[1,2,#], **Menghao Huang**[1,#], **Hyeong-Geug Kim**[1], **Kushan Chowdhury**[1], **Jing Gao**[1,3], **Sheng Liu**[4,5], **Jun Wan**[4,5], **Li Wei**[2,*], **X. Charlie Dong**[1,5,*]

[1]Department of Biochemistry and Molecular Biology, Indiana University School of Medicine, 635 Barnhill Drive, Indianapolis, IN 46202, USA

[2]Department of Endocrinology and Metabolism, Shanghai Jiao Tong University Affiliated Sixth People's Hospital, 600 Yishan Road, Shanghai 200233, China

[3]College of Food Science and Nutritional Engineering, China Agricultural University, 17 Qinghua Donglu, Beijing 100083, China

[4]Department of Medical and Molecular Genetics, Indiana University School of Medicine, Indianapolis, IN 46202, USA

[5]Center for Computational Biology and Bioinformatics, Indiana University School of Medicine, Indianapolis, IN 46202, USA

Abstract

Fatty liver disease is the most prevalent chronic liver disorder, which is manifested by hepatic triglyceride elevation, inflammation, and fibrosis. Sirtuin 6 (Sirt6), an NAD^+-dependent deacetylase, has been implicated in hepatic glucose and lipid metabolism; however, the underlying mechanisms are incompletely understood. The aim of this study was to identify and characterize novel players and mechanisms that are responsible for the Sirt6-mediated metabolic regulation in the liver. We generated and characterized Sirt6 liver-specific knockout mice regarding its role in the development of fatty liver disease. We used cell models to validate the molecular alterations observed in the animal models. Biochemical and molecular biological approaches were used to illustrate protein-protein interactions and gene regulation. Our data show that Sirt6 liver-specific knockout mice develop more severe fatty liver disease than wild-type mice do on a Western diet. Hepatic Sirt6 deficiency leads to elevated levels and transcriptional activities of carbohydrate response element binding protein (ChREBP) and sterol regulatory element binding

[*]**Corresponding authors:** X. Charlie Dong, PhD, Department of Biochemistry and Molecular Biology, Indiana University School of Medicine, 635 Barnhill Drive, MS-1021D, Indianapolis, IN 46202, USA, Phone: +1 317-278-1097, xcdong@iu.edu; Li Wei, MD, Department of Endocrinology and Metabolism, Shanghai Jiao Tong University Affiliated Sixth People's Hospital, 600 Yishan Road, Shanghai 200233, China, weili63@hotmail.com.

[#]Contributing equally to this work.

Author contribution statement

CZ – acquisition of data; analysis and interpretation of data; drafting of the manuscript. MH – acquisition of data; analysis and interpretation of data; drafting of the manuscript. HGK – acquisition of data; analysis and interpretation of data; drafting of the manuscript. KC – acquisition of data. JG – acquisition of data. SL – acquisition of data. JW – analysis and interpretation of data. LW - analysis and interpretation of data. XCD – study concept and design; analysis and interpretation of data; drafting of the manuscript; statistical analysis; obtaining funding; study supervision.

Conflict of interest statement

The authors have no conflict of interest.

protein 1 (SREBP1). Mechanistically, our data reveal protein-protein interactions between Sirt6 and liver X receptor α (LXRα), ChREBP, or SREBP1c in hepatocytes. Moreover, Sirt6 suppresses transcriptional activities of LXRα, ChREBP, and SREBP1c through direct deacetylation. In conclusion, this work has identified a key mechanism that is responsible for the salutary function of Sirt6 in the inhibition of hepatic lipogenesis by suppressing LXR, ChREBP, and SREBP1.

Graphical Abstract

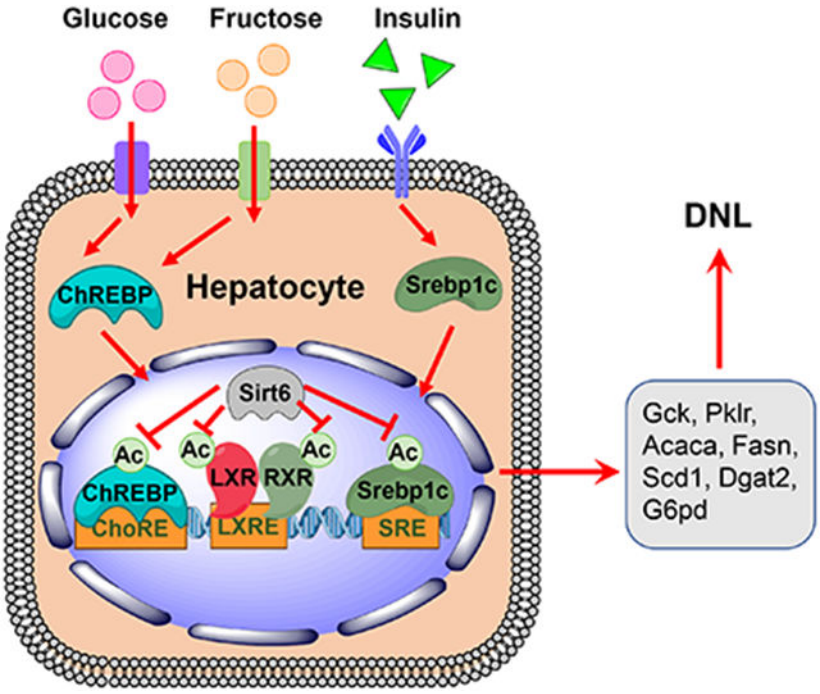

Keywords

Sirtuin; LXR; ChREBP; SREBP1; fatty liver; deacetylation

1. Introduction

Nonalcoholic fatty liver disease (NAFLD) is the most common chronic liver disorder in the world. NAFLD affects approximately 30% of the US population [1]. Hepatic lipid dysregulation is a key contributor to the development of NAFLD [2]. Hepatic lipid overload, especially elevated lipotoxic lipids, can cause liver injury and inflammation through multiple triggers including reactive oxygen species, endoplasmic reticulum (ER) stress, and damage-associated molecular patterns [2]. Hepatic triglyceride homeostasis is controlled by multiple processes including lipid transport from dietary fat intake and adipose tissue lipolysis, de novo lipogenesis, very low-density lipoprotein secretion, and hepatic lipid droplet breakdown and fatty acid oxidation [3]. Hepatic lipogenesis is regulated by several master regulators including liver X receptor (LXR), carbohydrate response element binding protein (ChREBP), and sterol regulatory element-binding protein 1 (SREBP1) [4]. LXRα/β can be activated by glucose, lipid and cholesterol intermediates, and they play a

critical role in glucose and lipid homeostasis [5]. *ChREBP* and *SREBP1* are among the key target genes of LXRα/β in the regulation of hepatic lipogenesis [5]. ChREBP is highly expressed in the liver and adipose tissues. In response to carbohydrate intake, ChREBP is activated by glucose and glucose metabolites, and subsequently translocates to the nucleus to promote transcription of numerous lipogenic genes including pyruvate kinase L/R (*PKLR*), acetyl-CoA carboxylase alpha (*ACACA*), and fatty acid synthase (*FASN*) [6]. SREBP1c, an isoform of SREBP1, is highly expressed in the liver, and it is processed from the precursor to mature form in the Golgi apparatus and translocates to the nucleus for transcription of target genes including lipogenic genes including *ACACA, FASN*, and stearoyl-CoA desaturase 1 (*SCD1*) in response to insulin stimulation [7].

Sirtuin 6 (Sirt6) is a member of the sirtuin family, which has been suggested to play a critical role in metabolic homeostasis, especially glucose and lipid metabolism [8]. Sirt6 has been shown to protect against alcoholic and non-alcoholic fatty liver diseases through suppression of oxidative stress, ER stress, and fibrosis [9–14]. Hepatic Sirt6 deficiency leads to elevated expression of glycolytic (glucokinase – *Gck* and *Pklr*) and lipogenic (*Acaca, Fasn, Scd1*, and ELOVL fatty acid elongase 6 – *Elovl6*) genes and decreased expression of fatty acid oxidation (carnitine palmitoyltransferase 1a – *Cpt1a* and acyl-CoA oxidase 1 – *Acox1*) genes in mouse livers [15]. However, the underlying mechanisms other than histone deacetylation are incompletely understood. In this work, we examined the role of Sirt6 in the regulation of hepatic lipogenesis through potential interactions with several master regulators including LXR, ChREBP, and SREBP1.

2. Materials and Methods

2.1. Animals

All animal care and experimental procedures performed in this study were approved by the Institutional Animal Care and Use Committee of Indiana University School of Medicine in accordance with the National Institutes of Health guidelines for the care and use of laboratory animals. *Sirt6* liver-specific knockout mice were generated by crossing *Sirt6* floxed mice with albumin-Cre transgenic mice as previously described [10]. Animals were fed either a control diet (Teklad Diets 2018SX: 24% calories from protein, 18% calories from fat, and 58% calories from carbohydrate), or moderately-high-fat-high-fructose-cholesterol diet (HFFC; Research Diets D18021203: 20% calories from protein, 40% calories from fat, 40% calories from carbohydrate and 1% cholesterol) for 11 weeks. Both males and females were used in the experiments and they were on the mixed background (C57BL/6J and 129/sv). At the end, the animals were euthanized for blood and tissue collection in the afternoon after 4 hours of fasting. Since the phenotypes were similar in males and females, the data presented here were primarily from the male mice.

2.2. Plasmid Construction and Mutagenesis

The coding sequences for human *SIRT6, SIRT6(H133Y)*, SMAD family member 3 (*SMAD3)*, retinoid X receptor alpha (*RXRα)*, mouse *ChREBP*, Srebp1c, *Lxrα*, and GFP were cloned into a pcDNA3 vector (Invitrogen) with a Flag or hemagglutinin (HA) tag by PCR cloning. *ChREBP, Srebp1c, Lxrα* and *RXRα* lysine-to-arginine mutants

were generated using a Q5 Site-Directed Mutagenesis Kit (New England Biolabs). DNA oligonucleotides were described in Table S1.

2.3. Cell Culture

Huh7 cells were cultured in Dulbecco's Modified Eagle medium (DMEM) supplemented with 10% fetal bovine serum (FBS) and penicillin/streptomycin (Thermo Fisher Scientific). SIRT6-deficient Huh7 cells were generated by CRISPR/Cas9 as we described previously [16]. Primary mouse hepatocytes were isolated as previously described [10]. Freshly isolated primary hepatocytes were seeded in a 6-well plate at 0.5 $x10^6$/well with DMEM plus 10% FBS.

2.4. mRNA Analysis

Total RNAs were isolated from tissues or cells using the TRI reagent (MilliporeSigma) and cDNAs were made using a cDNA synthesis kit (Applied Biosystems). Real-time PCR was performed using SYBR Green Master Mix (Applied Biosystems) in an Eppendorf Realplex PCR system. PCR data were analyzed using the $2^{-\Delta\Delta CT}$ method, and all quantifications were normalized to an internal control gene, peptidylprolyl isomerase A (PPIA). PCR primers used in this study were described in Table S1.

2.5. Blood Chemistry and Hepatic Triglyceride Analysis

Hepatic lipids were extracted from liver tissues using a chloroform-methanol extraction protocol as previously described [17]. Triglycerides, alanine aminotransferase and aspartate aminotransferase levels were analyzed using commercial assay kits from FUJIFILM Medical Systems USA and Thermo Fisher Scientific.

2.6. Microscopy Analysis

Huh7 cells were grown in a glass-bottom dish and then fixed with 4% paraformaldehyde for 15 min in room temperature, followed by washing 3 times with phosphate-buffered saline (PBS), and incubating in 0.1 mg/ml BODIPY solution for 30 min in the dark. After washing 3 times with PBS, cells were mounted with the Prolong Gold antifade mountant with 4′,6-diamidino-2-phenylindole (Invitrogen). Images were captured using a Zeiss Axio Observer Z1 fluorescence microscope (Zeiss USA, Thornwood, NY). Liver sections (4-μm thickness) were stained with hematoxylin and eosin (H&E) or Sirius Red stain (MilliporeSigma). For immunofluorescence analysis of hepatic inflammation and fibrosis, liver sections were deparaffinized, rehydrated, and then incubated with blocking buffer (2.5 % normal house serum) for one hour at room temperature, followed by an incubation with primary antibodies against F4/80 (1:250, Invitrogen) or Col1 (1:100, Abcam) at 4 °C overnight. Next, fluorophore-conjugated secondary antibodies were applied to the tissue sections. Images for H&E or Sirius Red staining were captured using a Leica microscope (100x or 200x total magnification). Immunofluorescent images were obtained using the Zeiss fluorescence microscope with an AxioVision Rel 4.8 software. Lipid droplet areas, Sirius Red–positive staining areas, and immunofluorescence-positive signals were quantified from randomly selected sections at least five fields per section using an Image J 1.52 software. The information of the antibodies used here was described in Table S2.

2.7. Immunoblot and Immunoprecipitation Analyses

Immunoblotting and immunoprecipitation analyses were performed as previously described [17]. Mouse tissues and cells were homogenized in either Triton X-100 lysis buffer (50 mM Hepes, pH 7.5, 150 mM NaCl, 10% Glycerol, 1% Triton X-100, 1.5 mM $MgCl_2$, 1 mM EDTA, 10 mM Sodium Pyrophosphate, 100 mM Sodium Fluoride, and freshly added 100 μM Sodium Vanadate, 1 mM PMSF, and 1x cOmplete protease inhibitor cocktail (Roche)) or NP-40 lysis buffer (1% NP-40, 20 mM Tris, pH 7.4, 137 mM NaCl, 2 mM EDTA, 10% Glycerol, 1 mM PMSF, and 1x cOmplete protease inhibitor cocktail). Equal amounts of protein lysates were resolved by SDS-PAGE and transferred to nitrocellulose membrane for Western blot analysis using specific antibodies. For quantitative analysis, enhanced chemiluminescence signals on immunoblots were analyzed by Gelpro32 Software (Media Cybernetics, Marlow, UK). For immunoprecipitations, equal amounts of protein extracts were incubated with 2 μg of anti-Flag antibody or 30μl of Anti-Flag M2 Affinity gel (MilliporeSigma) for 16 hours at 4°C. When the anti-Flag antibody was used for immunoprecipitation, protein A/G plus agarose beads (Santa Cruz Biotechnology, Dallas, TX) were added for a 3-hour incubation at 4°C. Normal rabbit or mouse IgG was used as a negative control. Immunoprecipitated proteins were analyzed by immunoblotting. Antibodies used here were described in Table S2.

2.8. Statistical Analysis

All statistical data were expressed as mean ± SEM. Statistical analysis was performed using the Prism 9 software from GraphPad (La Jolla, CA). Comparisons between two groups were performed using two-tailed unpaired Student t-test and comparisons for more than two groups were performed using one-way or two-way ANOVA followed by Tukey post-hoc tests.

3. Results

3.1 Key lipogenic transcription factors are elevated whereas Sirt6 is downregulated in the liver of high-fat diet fed mice

To assess the effect of Western diet on key lipogenic regulators, we fed wild-type (WT) C57BL6/J mice with a control or HFFC diet for 11 weeks and analyzed expression of Sirt6, Lxrα/β, ChREBP, and Srebp1 precursor (pSrebp1) and mature form (mSrebp1) in the livers. Hepatic Sirt6 protein was decreased 50% in the HFFC-fed mice whereas hepatic Lxrα/β, ChREBP, and mSrebp1 protein levels were significantly increased (Fig. 1A, B). To further verify whether the changes in these proteins occur in hepatocytes, we also performed immunoblot analysis of primary hepatocytes isolated from WT mice fed with a control or HFFC diet for 4 weeks. The hepatocyte data were consistent with the liver data. Hepatic Sirt6 was decreased and Lxrα/β, ChREBP, and mSrebp1 proteins were increased in the HFFC diet fed mice compared to the control diet fed mice (Fig. 1C, D). In addition, real-time PCR data showed Sirt6 mRNA levels were decreased whereas ChREBP, Srebp1c, and Lxrα mRNA levels were increased in the primary hepatocytes from the HFFC-treated mice compared to controls. As expected, glycolytic and lipogenic genes such as *Gck, Fasn*, and *Scd1* were upregulated in the HFFC-treated mouse hepatocytes (Fig. 1E, F).

3.2 Hepatic Sirt6 deficiency makes mice susceptible to diet-induced NAFLD

To further investigate the role of Sirt6 in Western diet-induced NAFLD, we subjected WT and liver-specific *Sirt6* knockout mice (LKO; Alb-Cre-mediated) to a control or HFFC diet. As shown by immunoblot analysis, *Sirt6* was deleted specifically in the liver but not skeletal muscle of the LKO mice (Fig. 2A). After treatment with the HFFC diet for 11 weeks, WT mice developed a typical fatty liver phenotype whereas LKO mice manifested a more severe phenotype with paler and larger livers even though body weights were not different (Fig. 2B–E and Fig. 3A). Hematoxylin and eosin staining and lipid droplet quantification confirmed a more severe hepatic steatosis in the LKO mice than that in the WT mice (Fig. 2E and Fig. 3A). Moreover, biochemical analysis also showed that serum and hepatic triglycerides and diacylglycerol were increased by 33%, 37%, and 58% in the LKO mice relative to the WT mice on the HFFC diet, respectively (Fig. 2F–H).

Next, we assessed hepatic inflammation by immunofluorescence staining a macrophage marker – F4/80. Hepatic macrophage numbers were significantly increased in HFFC-treated LKO mice compared to WT mice (Fig. S1A, B). We also examined hepatic fibrosis by Sirius Red staining and Col1 immunofluorescence microscopy. Both fibrosis indicators were elevated in the HFFC-treated LKO livers compared to the WT livers (Fig. S1A, C, D). In line with hepatic inflammation, serum alanine aminotransferase (ALT) and aspartate aminotransferase (AST) levels were increased by 90% and 92% in the HFFC-treated LKO mice relative to the WT mice (Fig. S1E, F). Hepatic inflammation and fibrosis were also corroborated by induction of inflammatory and fibrogenic genes including interleukin 1b (*Il1b)*, tumor necrosis factor *(Tnf)*, C-C motif chemokine ligand 2 (*Ccl2)*, collagen type I alpha 1 chain (*Col1a1)*, collagen type IV alpha 1 chain (*Col4a1)*, smooth muscle actin alpha 2 (*Acta2)*, transforming growth factor beta 1 *(Tgfb1)*, and connective tissue growth factor (*Ctgf)* in the HFFC-treated livers (Fig. S1G, H).

3.3 Sirt6 deficiency leads to dysregulation of hepatic glycolytic and lipogenic genes

To assess the effect of hepatic Sirt6 deficiency on metabolic regulation, we analyzed three key regulators for lipogenesis – Srebp1, ChREBP, and Lxr in the livers of WT and LKO mice fed with the HFFC diet for 11 weeks. Interestingly, the protein levels of mSrebp1 and ChREBP were remarkably elevated whereas Lxrα/β protein levels were not altered in the livers of the HFFC-treated LKO mice compared to the HFFC-treated WT mice (Fig. 3B). Real-time PCR analysis showed that *Srebp1c and ChREBP* (including α and β isoforms) mRNA levels also significantly increased whereas *Lxrα* mRNA levels were not altered in the HFFC-treated LKO livers compared to the HFFC-treated WT livers (Fig. 3C). In addition, we analyzed multiple glycolytic and lipogenic genes including *Gck, Pklr, Fasn, Acaca, Scd1*, and diacylglycerol O-acyltransferase 2 (*Dgat2)*. These genes were induced by the HFFC diet in the WT mouse livers and even more so in the LKO livers (Fig. 3D). Systemic insulin resistance and glucose intolerance were assessed by insulin and glucose tolerance tests. The data showed that LKO mice exhibited worsened glucose intolerance and insulin resistance as compared to their WT counterparts (Fig. 3E, F).

As bile acids play a critical role in hepatic metabolism and NAFLD [18], we also analyzed expression of several genes that are involved in bile acid biosynthesis (*Cyp7a1*,

cytochrome P450 family 7 subfamily A member 1; *Cyp7b1*, cytochrome P450 family 7 subfamily B member 1; *Cyp8b1*, cytochrome P450 family 8 subfamily B member 1; Cyp27a1, cytochrome P450 family 27 subfamily A member 1), transport (*Abcb11*, ATP binding cassette subfamily B member 11, also named *Bsep*, bile salt export pump; *Slc10a1*, solute carrier family 10 member 1, also named *Ntcp*, sodium/taurocholate cotransporting polypeptide; *Slco1a2*, solute carrier organic anion transporter family member 1A2, also named *Oatp1*, organic anion transporting polypeptide 1; and Abcc3/4, ATP binding cassette subfamily C members 3/4, also named MRP3/4, multidrug resistance associated protein 3/4), and regulation (*Nr0b2*, nuclear receptor subfamily 0 group B member 2, also named *Shp*, small heterodimer partner; *Nr1h4*, nuclear receptor subfamily 1 group H member 4, also named *Fxr*, farnesoid X receptor). On the HFFC diet, mRNA levels of the *Cyp7a1, Slco1a2*, and *Abcc4* genes were increased whereas mRNA levels of the *Cyp7b1, Cyp27a1, Abcb11, Abcc3, Nr0b2*, and *Nr1h4* genes were decreased in the liver of the Sirt6-LKO mice compared to WT mice (Fig. S2A, B), suggesting that the classic and alternative pathways for the bile acid biosynthesis are differentially regulated in the Sirt6-LKO liver. Regarding the bile acid transport, the gene expression data seems to suggest that the Abcb11-mediated canalicular efflux may be decreased whereas the Slco1a2-mediated uptake into hepatocytes may be increased. The other two efflux transporters Abcc3 and Abcc4 had mixed trends on their mRNA levels. The downregulation of both Fxr and Shp also suggests an impairment in the feedback regulation by bile acids in the Sirt6-LKO liver. Additionally, expression of three bile duct related genes – keratin 19 (*Krt19)*, epithelial cell adhesion molecule *(Epcam)*, and SRY-box transcription factor 9 *(Sox9)* – was increased at the mRNA levels in the HFFC-treated Sirt6-LKO livers as compared to the WT controls (Fig. S2C). This suggests that ductular reaction is likely in the liver of the Sirt6-LKO mice.

Ceramides have been implicated in hepatic insulin resistance and NAFLD [19]. Therefore, we also surveyed genes in the ceramide metabolic pathway using real-time PCR analysis. Interestingly, expression of several genes involved in the ceramide biosynthesis including serine palmitoyltransferase long chain base subunit 2 (*Sptlc2*), 3-ketodihydrosphingosine reductase (*Kdsr*), ceramide synthases 2 and 6 (*Cers2* and *Cers6*), and dihydroceramide desaturase 1 (*Degs1*) was increased at the mRNA levels. However, expression of genes involved in the ceramide metabolism, particularly for sphingosine, sphingosine-1-phosphate, and hexadecanal and phosphoethanolamine, had mixed directions. For the conversion from ceramide to sphingosine, both N-acylsphingosine amidohydrolases 1 and 2 (*Asah1* and *Asah2*) were decreased at the mRNA levels in the HFFC-treated Sirt6-LKO livers (Fig. S2D). For the downstream reactions from sphingosine, sphingosine kinase 1 (*Sphk1*) and sphingosine-1-phosphate lyase 1 (*Sgpl1*) were increased at the mRNA levels in the HFFC-treated Sirt6-LKO livers (Fig. S2D). An enzyme for conversion of sphingomyelin to ceramide – sphingomyelin phosphodiesterase 1 (Smpd1) – was markedly elevated at mRNA levels whereas an enzyme for the reverse reaction – sphingomyelin synthase 2 (Sgms2) – had no significant change in the Sirt6-LKO livers as compared to the WT livers on both control and HFFC diets (Fig. S2D). These data suggest that the ceramide biosynthesis may be increased and the conversion from ceramide to sphingosine may be decreased in the Sirt6-LKO liver on the HFFC diet.

3.4. Sirt6 downregulates ChREBP and SREBP1 at multiple levels

To further investigate the molecular mechanism that is responsible for the suppression of hepatic lipogenesis by SIRT6, we performed both loss-of-function and gain-of-function analyses for SIRT6 in Huh7 human hepatocyte cell line. First, we generated stable *SIRT6* knockdown in Huh7 using the CRISPR-Cas9 method. As expected, *SIRT6* knockdown increased neutral lipid accumulation evidenced by BODIPY staining (Fig. 4A). pSREBP1, mSREBP1, LXRα/β, and ChREBP protein levels were increased in the SIRT6 knockdown hepatocytes compared to WT cells (Fig. 4B). SREBP1c and ChREBP mRNA levels were also increased in the SIRT6-deficient cells as compared to WT cells (Fig. 4C). Several SREBP1 target genes including lipin 1 (*LPIN1), SCD1*, and *ELOVL5* and ChREBP target genes such as *SCD1*, fibroblast growth factor 21 (*FGF21), PKLR*, and glucose-6-phosphate dehydrogenase (*G6PD*) were also upregulated in the *SIRT6* knockdown hepatocytes relative to controls (Fig. 4D). Second, we overexpressed *SIRT6* in Huh7 cells. Overexpression of SIRT6 reduced neutral lipid levels as predicted (Fig. 4E). SREBP1 and ChREBP protein levels were decreased in the *SIRT6* overexpressing cells compared to vector controls (Fig. 4F). Real-time PCR analysis also revealed that mRNA levels of SREBP1c and ChREBP and their target genes were decreased in the *SIRT6* overexpressing cells compared to controls (Fig. 4G, H).

To further assess whether SIRT6 directly interacts with SREBP1, ChREBP, or LXR, we performed co-immunoprecipitation analyses in Huh7 cells. First, we co-transfected cells with Flag-tagged GFP (a negative control), SMAD3 (a positive control), LXRα, or RXRα together with HA-tagged SIRT6 and immunoprecipitated proteins with Flag antibody beads. Our data showed that LXRα and RXRα interacted with SIRT6, respectively (Fig. 5A). Second, using the same approach, we confirmed that SIRT6 also interacted with ChREBP and SREBP1, respectively (Fig. 5B, C). Third, we used Flag-tagged SIRT6 to successfully pull down endogenous LXRα, SREBP1, and ChREBP proteins (Fig. 5D).

To further analyze whether SIRT6 deacetylates SREBP1, ChREBP, LXRα, or RXRα, we overexpressed wild-type or catalytically inactive mutant SIRT6 (H133Y) and examined total acetylation levels of these proteins. Our data showed that wild-type SIRT6 but not mutant SIRT6 reduced the acetylation levels of SREBP1, ChREBP, LXRα, and RXRα (Fig. 6A), suggesting that the catalytic activity of SIRT6 is required for the deacetylation. To narrow down specific lysine residues in these proteins that are potential catalytic sites of SIRT6, we selected several previously identified lysine (K) sites in LXRα, RXRα, SREBP1, and ChREBP [20–23], and mutated them to arginine that cannot be acetylated. Our data showed that K432 of LXRα, K672 in ChREBP, and K289 in SREBP1c are potential deacetylation sites by SIRT6, respectively, whereas K150 in RXRα seemed not to be a substrate of SIRT6, as K432R, K672R, and K289R mutant proteins were no longer responsive to wild-type SIRT6 overexpression (Fig. 6B–E).

Next, we evaluated the role of deacetylation of those specific lysine residues in LXRα, RXRα, ChREBP, and SREBP1c in the regulation of their target genes in Huh7 cells using real-time PCR analysis. Our data showed that acetylation of K432 played a positive role in the LXRα regulation of multiple genes including *SREBP1c, ChREBP, ELOVL5, LPIN1, SCD1, PKLR, FGF21*, and *G6PD* as mutation of this lysine to arginine dramatically reduced

expression of these genes. Wild-type but not mutant SIRT6 markedly attenuated the LXRα effects on the regulation of those downstream genes (Fig. 7A–H). In line with the acetylation data on RXRα, gene expression data also suggested that K150 in RXRα does not seem to play a role in the SIRT6-regulated RXRα activity (Fig. S2A-H). K672R mutation of ChREBP did not affect the suppressive effect of SIRT6 on the *LPIN1* and *ELOVL5* genes, which are not ChREBP targets; however, the same mutation of ChREBP had a very profound effect on expression of *SCD1, PKLR, FGF21*, and *G6PD* genes, which are known ChREBP targets. Interestingly, SIRT6 showed an additional suppressive effect on those ChREBP targets on top of the K672 mutation, suggesting that additional acetylation sites may be involved in the SIRT6 regulation of ChREBP (Fig. 8A–F). Our data also showed that acetylation of K289 but not K309 in SREBP1c played a positive role in the regulation of *LPIN1, ELOVL5*, and *SCD1*, which are known SREBP1c targets, and K289R mutation reduced expression of these target genes but not others like *PKLR, FGF21*, and *G6PD*. On top of the K289R mutation, wild-type but not mutant SIRT6 could further attenuated expression of the SREBP1c target genes, suggesting that additional acetylation sites may be involved in the suppressive regulation of SREBP1c by SIRT6 (Fig. 8G–L).

4. Discussion

Sirt6 has been implicated in the regulation of multiple metabolic processes in the liver to protect against hepatic steatosis, inflammation, oxidative stress and fibrosis [9–15, 24–27]. Here in this work, we have identified a critical link from Sirt6 to key transcription factors involved in lipogenesis such as LXR, ChREBP, and SREBP1. This observation further supports the significant role of Sirt6 in hepatic lipid homeostasis. Moreover, our biochemical analysis has revealed a multi-layer regulatory mechanism. First, Sirt6 controls the LXR transcriptional activity. LXR is a master regulator of glucose and lipid metabolism, especially *de novo* lipogenesis, as ChREBP and SREBP1 are among the significant transcriptional targets of LXR [5, 28–36]. Second, Sirt6 also directly controls the transcriptional activities of ChREBP and SREBP1.

LXRα can be deacetylated at K432 by Sirt1, and this leads to activation and ubiquitin-mediated degradation LXRα [21]. This is in contrast to what we have observed on the regulation of LXRα by Sirt6 in this work. First, LXRα/β protein levels are not significantly changed in the Sirt6-LKO mouse livers as compared to a dramatic increase in the livers of Sirt1 whole-body knockout mice. Second, deacetylation of LXRα at K432 by Sirt6 suppresses the transcriptional activity of LXRα as compared to activation by Sirt1 through deacetylation of LXRα at the same lysine residue. Apparently, these differences raise questions regarding the nature of protein-protein interaction and the associated protein complex(es) brought upon by either Sirt1 or Sirt6. Further studies will be warranted to address those questions in the future.

ChREBP can be acetylated at K672 by histone acetyltransferase p300 and the acetylated ChREBP is more active in transcriptional activity [20]. In this work, we have demonstrated that Sirt6 deacetylates acetyl-K672 and thus suppresses the ChREBP transcriptional activity. SREBP1c can be acetylated at K289 and K309 by p300 and deacetylated by Sirt1. Deacetylated SREBP1c has reduced stability and transcriptional activity [22]. Our data

suggest that acetyl-K289 of SREBP1c but not acetyl-K309 is a substrate of Sirt6 and K289 deacetylation by Sirt6 significantly attenuates the SREBP1c transcriptional activity.

The data from this study suggest that Sirt6 is a critical regulator for controlling hepatic lipogenesis through suppression of LXR, ChREBP, and SREBP1c. Future studies are needed to further elucidate the environmental cues that impact the Sirt6 function on these and potentially other key regulators in hepatic lipid metabolism. Nevertheless, the findings to date suggest that Sirt6 is a potential candidate as therapeutic target for NAFLD.

Supplementary Material

Refer to Web version on PubMed Central for supplementary material.

Funding

This study was supported in part by the following funding sources: NIH R56DK091592 (X. Charlie Dong), NIH R21AA024550 (X. Charlie Dong), NIH R01DK120689 (X. Charlie Dong), NIH R01DK121925 (X. Charlie Dong), Indiana Clinical and Translational Sciences Institute funded by the NIH NCATS CTSA UL1TR002529, National Natural Science Foundation of China 81500615 (Chaoyu Zhu) and 81870603 (Li Wei). Dr. Chaoyu Zhu was a visiting scholar who was partially supported by the Shanghai Jiao Tong University Affiliated Sixth People's Hospital. Ms. Jing Gao was a visiting graduate student who was partially supported by a scholarship from the China Scholarship Council.

Abbreviations:

ABCB11	ATP binding cassette subfamily B member 11
ABCC3/4	ATP binding cassette subfamily C members 3/4
ACACA	acetyl-CoA carboxylase alpha
ACOX1	acyl-CoA oxidase 1
ACTA2	smooth muscle actin alpha 2
ALT	alanine aminotransferase
ASAH1/2	N-acylsphingosine amidohydrolase 1/2
AST	aspartate aminotransferase
BSEP	bile salt export pump
CCL2	C-C motif chemokine ligand 2
CERS2/6	ceramide synthase 2/6
ChREBP	carbohydrate response element binding protein
COL1A1	collagen type I alpha 1 chain
COL4A1	collagen type IV alpha 1 chain
CPT1A	carnitine palmitoyltransferase 1a

CTGF	connective tissue growth factor
CYP7A1	cytochrome P450 family 7 subfamily A member 1
CYP7B1	cytochrome P450 family 7 subfamily B member 1
CYP8B1	cytochrome P450 family 8 subfamily B member 1
CYP27A1	cytochrome P450 family 27 subfamily A member 1
DAG	diacylglycerol
DEGS1	dihydroceramide desaturase 1
DGAT2	diacylglycerol O-acyltransferase 2
ELOVL6	ELOVL fatty acid elongase 6
EPCAM	epithelial cell adhesion molecule
ER	endoplasmic reticulum
FASN	fatty acid synthase
FGF21	fibroblast growth factor 21
FXR	farnesoid X receptor
G6PD	glucose-6-phosphate dehydrogenase
GCK	glucokinase
HFFC	high-fat high-fructose plus cholesterol
IL1b	interleukin 1b
KDSR	3-ketodihydrosphingosine reductase
KRT19	keratin 19
LPIN1	lipin 1
LXR	liver X receptor
MRP3/4	multidrug resistance associated protein 3/4
NAFLD	nonalcoholic fatty liver disease
NR0B2	nuclear receptor subfamily 0 group B member 2
NR1H4	nuclear receptor subfamily 1 group H member 4
NTCP	sodium/taurocholate cotransporting polypeptide
OATP	organic anion transporting polypeptide
PKLR	pyruvate kinase L/R

PPIA	peptidylprolyl isomerase A
RXRα	retinoid X receptor alpha
SCD1	stearoyl-CoA desaturase 1
SGMS2	sphingomyelin synthase 2
SGPL1	sphingosine-1-phosphate lyase 1
SHP	small heterodimer partner
SIRT6	sirtuin 6
SLC10A1	solute carrier family 10 member 1
SLCO1A2	solute carrier organic anion transporter family member 1A2
SMPD1	sphingomyelin phosphodiesterase 1
SOX9	SRY-box transcription factor 9
SPHK1/2	sphingosine kinase 1/2
SPTLC1/2	serine palmitoyltransferase long chain base subunits 1/2
SREBP1	sterol regulatory element binding protein 1
TG	triglyceride
TGFB1	transforming growth factor beta 1
TNF	tumor necrosis factor

References

[1]. Cotter TG, Rinella M, Nonalcoholic Fatty Liver Disease 2020: The State of the Disease, Gastroenterology, 158 (2020) 1851–1864. [PubMed: 32061595]

[2]. Friedman SL, Neuschwander-Tetri BA, Rinella M, Sanyal AJ, Mechanisms of NAFLD development and therapeutic strategies, Nat Med, 24 (2018) 908–922. [PubMed: 29967350]

[3]. Neuschwander-Tetri BA, Therapeutic Landscape for NAFLD in 2020, Gastroenterology, 158 (2020) 1984–1998 e1983. [PubMed: 32061596]

[4]. Wang Y, Viscarra J, Kim SJ, Sul HS, Transcriptional regulation of hepatic lipogenesis, Nat Rev Mol Cell Biol, 16 (2015) 678–689. [PubMed: 26490400]

[5]. Wang B, Tontonoz P, Liver X receptors in lipid signalling and membrane homeostasis, Nat Rev Endocrinol, 14 (2018) 452–463. [PubMed: 29904174]

[6]. Ortega-Prieto P, Postic C, Carbohydrate Sensing Through the Transcription Factor ChREBP, Frontiers in genetics, 10 (2019) 472. [PubMed: 31275349]

[7]. Shimano H, Sato R, SREBP-regulated lipid metabolism: convergent physiology - divergent pathophysiology, Nat Rev Endocrinol, 13 (2017) 710–730. [PubMed: 28849786]

[8]. Chang AR, Ferrer CM, Mostoslavsky R, SIRT6, a Mammalian Deacylase with Multitasking Abilities, Physiol Rev, 100 (2020) 145–169. [PubMed: 31437090]

[9]. Zhang J, Li Y, Liu Q, Huang Y, Li R, Wu T, Zhang Z, Zhou J, Huang H, Tang Q, Huang C, Zhao Y, Zhang G, Jiang W, Mo L, Zhang J, Xie W, He J, Sirt6 Alleviated Liver Fibrosis by

Deacetylating Conserved Lysine 54 on Smad2 in Hepatic Stellate Cells, Hepatology, 73 (2021) 1140–1157. [PubMed: 32535965]

[10]. Zhong X, Huang M, Kim HG, Zhang Y, Chowdhury K, Cai W, Saxena R, Schwabe RF, Liangpunsakul S, Dong XC, SIRT6 Protects Against Liver Fibrosis by Deacetylation and Suppression of SMAD3 in Hepatic Stellate Cells, Cell Mol Gastroenterol Hepatol, 10 (2020) 341–364. [PubMed: 32305562]

[11]. Maity S, Muhamed J, Sarikhani M, Kumar S, Ahamed F, Spurthi KM, Ravi V, Jain A, Khan D, Arathi BP, Desingu PA, Sundaresan NR, Sirtuin 6 deficiency transcriptionally up-regulates TGF-beta signaling and induces fibrosis in mice, J Biol Chem, 295 (2020) 415–434. [PubMed: 31744885]

[12]. Hao L, Bang IH, Wang J, Mao Y, Yang JD, Na SY, Seo JK, Choi HS, Bae EJ, Park BH, ERRgamma suppression by Sirt6 alleviates cholestatic liver injury and fibrosis, JCI Insight, 5 (2020).

[13]. Kim HG, Huang M, Xin Y, Zhang Y, Zhang X, Wang G, Liu S, Wan J, Ahmadi AR, Sun Z, Liangpunsakul S, Xiong X, Dong XC, The epigenetic regulator SIRT6 protects the liver from alcohol-induced tissue injury by reducing oxidative stress in mice, J Hepatol, 71 (2019) 960–969. [PubMed: 31295533]

[14]. Bang IH, Kwon OK, Hao L, Park D, Chung MJ, Oh BC, Lee S, Bae EJ, Park BH, Deacetylation of XBP1s by sirtuin 6 confers resistance to ER stress-induced hepatic steatosis, Exp Mol Med, 51 (2019) 107.

[15]. Kim HS, Xiao C, Wang RH, Lahusen T, Xu X, Vassilopoulos A, Vazquez-Ortiz G, Jeong WI, Park O, Ki SH, Gao B, Deng CX, Hepatic-specific disruption of SIRT6 in mice results in fatty liver formation due to enhanced glycolysis and triglyceride synthesis, Cell Metab, 12 (2010) 224–236. [PubMed: 20816089]

[16]. Fang Z, Kim HG, Huang M, Chowdhury K, Li MO, Liangpunsakul S, Dong XC, Sestrin Proteins Protect Against Lipotoxicity-Induced Oxidative Stress in the Liver via Suppression of C-Jun N-Terminal Kinases, Cell Mol Gastroenterol Hepatol, (2021).

[17]. Huang M, Kim HG, Zhong X, Dong C, Zhang B, Fang Z, Zhang Y, Lu X, Saxena R, Liu Y, Zhang C, Liangpunsakul S, Dong XC, Sestrin 3 Protects Against Diet-Induced Nonalcoholic Steatohepatitis in Mice Through Suppression of Transforming Growth Factor beta Signal Transduction, Hepatology, 71 (2020) 76–92. [PubMed: 31215672]

[18]. Chow MD, Lee YH, Guo GL, The role of bile acids in nonalcoholic fatty liver disease and nonalcoholic steatohepatitis, Mol Aspects Med, 56 (2017) 34–44. [PubMed: 28442273]

[19]. Chaurasia B, Summers SA, Ceramides in Metabolism: Key Lipotoxic Players, Annu Rev Physiol, 83 (2021) 303–330. [PubMed: 33158378]

[20]. Bricambert J, Miranda J, Benhamed F, Girard J, Postic C, Dentin R, Salt-inducible kinase 2 links transcriptional coactivator p300 phosphorylation to the prevention of ChREBP-dependent hepatic steatosis in mice, J Clin Invest, 120 (2010) 4316–4331. [PubMed: 21084751]

[21]. Li X, Zhang S, Blander G, Tse JG, Krieger M, Guarente L, SIRT1 deacetylates and positively regulates the nuclear receptor LXR, Mol Cell, 28 (2007) 91–106. [PubMed: 17936707]

[22]. Ponugoti B, Kim DH, Xiao Z, Smith Z, Miao J, Zang M, Wu SY, Chiang CM, Veenstra TD, Kemper JK, SIRT1 deacetylates and inhibits SREBP-1C activity in regulation of hepatic lipid metabolism, J Biol Chem, 285 (2010) 33959–33970. [PubMed: 20817729]

[23]. Zhao WX, Tian M, Zhao BX, Li GD, Liu B, Zhan YY, Chen HZ, Wu Q, Orphan receptor TR3 attenuates the p300-induced acetylation of retinoid X receptor-alpha, Mol Endocrinol, 21 (2007) 2877–2889. [PubMed: 17761950]

[24]. Naiman S, Huynh FK, Gil R, Glick Y, Shahar Y, Touitou N, Nahum L, Avivi MY, Roichman A, Kanfi Y, Gertler AA, Doniger T, Ilkayeva OR, Abramovich I, Yaron O, Lerrer B, Gottlieb E, Harris RA, Gerber D, Hirschey MD, Cohen HY, SIRT6 Promotes Hepatic Beta-Oxidation via Activation of PPARalpha, Cell reports, 29 (2019) 4127–4143 e4128. [PubMed: 31851938]

[25]. Tao R, Xiong X, DePinho RA, Deng CX, Dong XC, FoxO3 transcription factor and Sirt6 deacetylase regulate low density lipoprotein (LDL)-cholesterol homeostasis via control of the proprotein convertase subtilisin/kexin type 9 (Pcsk9) gene expression, J Biol Chem, 288 (2013) 29252–29259. [PubMed: 23974119]

[26]. Tao R, Xiong X, DePinho RA, Deng CX, Dong XC, Hepatic SREBP-2 and cholesterol biosynthesis are regulated by FoxO3 and Sirt6, J Lipid Res, 54 (2013) 2745–2753. [PubMed: 23881913]

[27]. Xiao C, Wang RH, Lahusen TJ, Park O, Bertola A, Maruyama T, Reynolds D, Chen Q, Xu X, Young HA, Chen WJ, Gao B, Deng CX, Progression of Chronic Liver Inflammation and Fibrosis Driven by Activation of c-JUN Signaling in Sirt6 Mutant Mice, J Biol Chem, 287 (2012) 41903–41913. [PubMed: 23076146]

[28]. Cha JY, Repa JJ, The liver X receptor (LXR) and hepatic lipogenesis. The carbohydrate-response element-binding protein is a target gene of LXR, J Biol Chem, 282 (2007) 743–751. [PubMed: 17107947]

[29]. Chen G, Liang G, Ou J, Goldstein JL, Brown MS, Central role for liver X receptor in insulin-mediated activation of Srebp-1c transcription and stimulation of fatty acid synthesis in liver, Proc Natl Acad Sci U S A, 101 (2004) 11245–11250. [PubMed: 15266058]

[30]. Joseph SB, Laffitte BA, Patel PH, Watson MA, Matsukuma KE, Walczak R, Collins JL, Osborne TF, Tontonoz P, Direct and indirect mechanisms for regulation of fatty acid synthase gene expression by liver X receptors, J Biol Chem, 277 (2002) 11019–11025. [PubMed: 11790787]

[31]. Peet DJ, Turley SD, Ma W, Janowski BA, Lobaccaro JM, Hammer RE, Mangelsdorf DJ, Cholesterol and bile acid metabolism are impaired in mice lacking the nuclear oxysterol receptor LXR alpha, Cell, 93 (1998) 693–704. [PubMed: 9630215]

[32]. Quinet EM, Savio DA, Halpern AR, Chen L, Miller CP, Nambi P, Gene-selective modulation by a synthetic oxysterol ligand of the liver X receptor, J Lipid Res, 45 (2004) 1929–1942. [PubMed: 15292374]

[33]. Repa JJ, Liang G, Ou J, Bashmakov Y, Lobaccaro JM, Shimomura I, Shan B, Brown MS, Goldstein JL, Mangelsdorf DJ, Regulation of mouse sterol regulatory element-binding protein-1c gene (SREBP-1c) by oxysterol receptors, LXRalpha and LXRbeta, Genes Dev, 14 (2000) 2819–2830. [PubMed: 11090130]

[34]. Schultz JR, Tu H, Luk A, Repa JJ, Medina JC, Li L, Schwendner S, Wang S, Thoolen M, Mangelsdorf DJ, Lustig KD, Shan B, Role of LXRs in control of lipogenesis, Genes Dev, 14 (2000) 2831–2838. [PubMed: 11090131]

[35]. Venkateswaran A, Laffitte BA, Joseph SB, Mak PA, Wilpitz DC, Edwards PA, Tontonoz P, Control of cellular cholesterol efflux by the nuclear oxysterol receptor LXR alpha, Proc Natl Acad Sci U S A, 97 (2000) 12097–12102. [PubMed: 11035776]

[36]. Yoshikawa T, Shimano H, Amemiya-Kudo M, Yahagi N, Hasty AH, Matsuzaka T, Okazaki H, Tamura Y, Iizuka Y, Ohashi K, Osuga J, Harada K, Gotoda T, Kimura S, Ishibashi S, Yamada N, Identification of liver X receptor-retinoid X receptor as an activator of the sterol regulatory element-binding protein 1c gene promoter, Mol Cell Biol, 21 (2001) 2991–3000. [PubMed: 11287605]

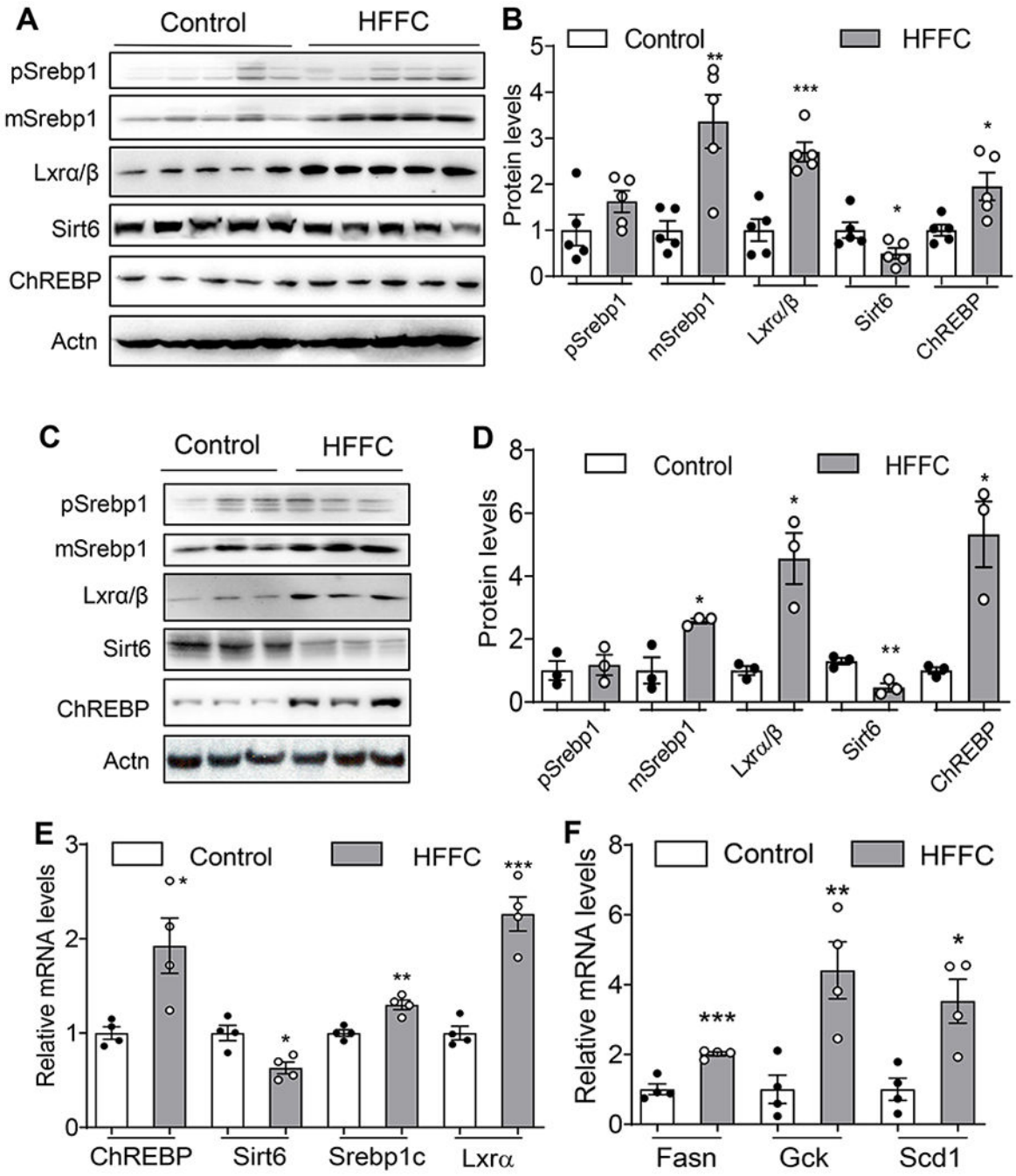

Figure 1. Sirt6 is decreased and key lipogenic regulators are increased in the liver of a diet-induced NAFLD mouse model.

(A, B) Western blot and quantification analysis of Sirt6, Lxrα/β, ChREBP, and Srebp1 precursor and mature forms (pSrebp1 and mSrebp1, respectively) in the livers of WT male mice (n=5) fed with a control or HFFC diet for 11 weeks. (C, D) Western blot and quantification analysis of Sirt6, Lxrα/β, ChREBP, and Srebp1 in primary hepatocytes of WT male mice fed with a control or HFFC diet for 4 weeks (n=3). (E, F) Real-time PCR analysis of *ChREBP, Sirt6, Srebp1c, Lxrα, Fasn, Gck*, and *Scd1* in the primary hepatocytes isolated

from livers of WT male mice fed with the control or HFFC diet for 4 weeks (n=3). Data are presented as mean ± SEM. *p < 0.05, **p < 0.01 and ***p < 0.001.

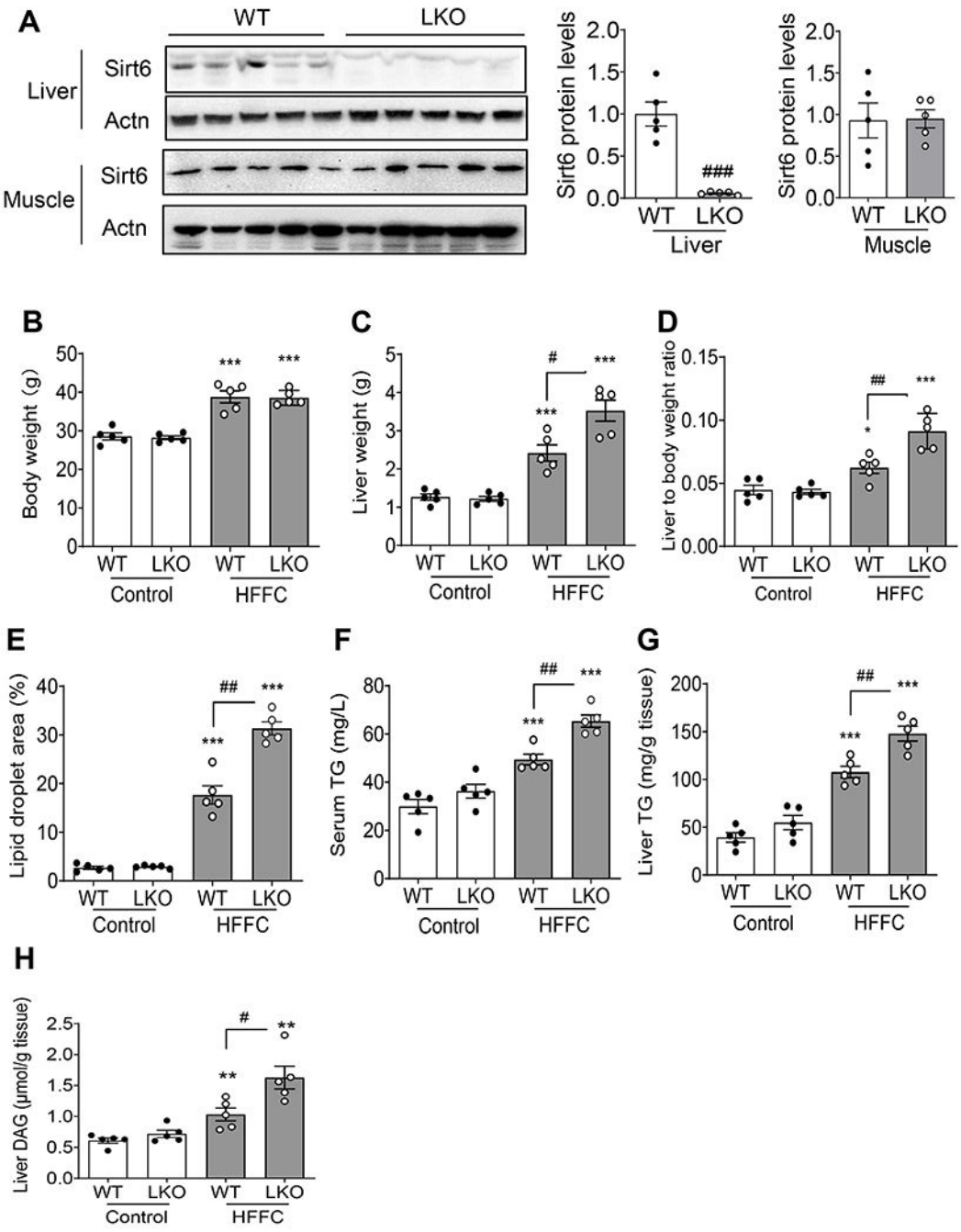

Figure 2. Sirt6 liver-specific knockout mice are more susceptible to diet-induced hepatic steatosis.

(A) Western blot and quantification analysis of Sirt6 in the liver and muscle of WT and Sirt6-LKO male mice fed with a HFFC diet for 11 weeks (n=4). (B-D) Body weight, liver weight, and liver to body weight ratios of WT and Sirt6-LKO male mice fed with the control or HFFC diet for 11 weeks (n=5). (E) Lipid droplet area analysis of liver sections of WT and Sirt6-LKO male mice fed with the control or HFFC diet for 11 weeks (n=5). (F-H) Serum and hepatic triglycerides (TG) and hepatic diacylglycerol (DAG) levels in WT and Sirt6-LKO male mice fed with the control or HFFC diet for 11 weeks (n=5). Data are

presented as mean ± SEM. *p < 0.05, and ***p < 0.001 for HFFC vs. control for the same genotype; #p < 0.05, ##p < 0.01, and ###p < 0.001 vs. WT for the same diet.

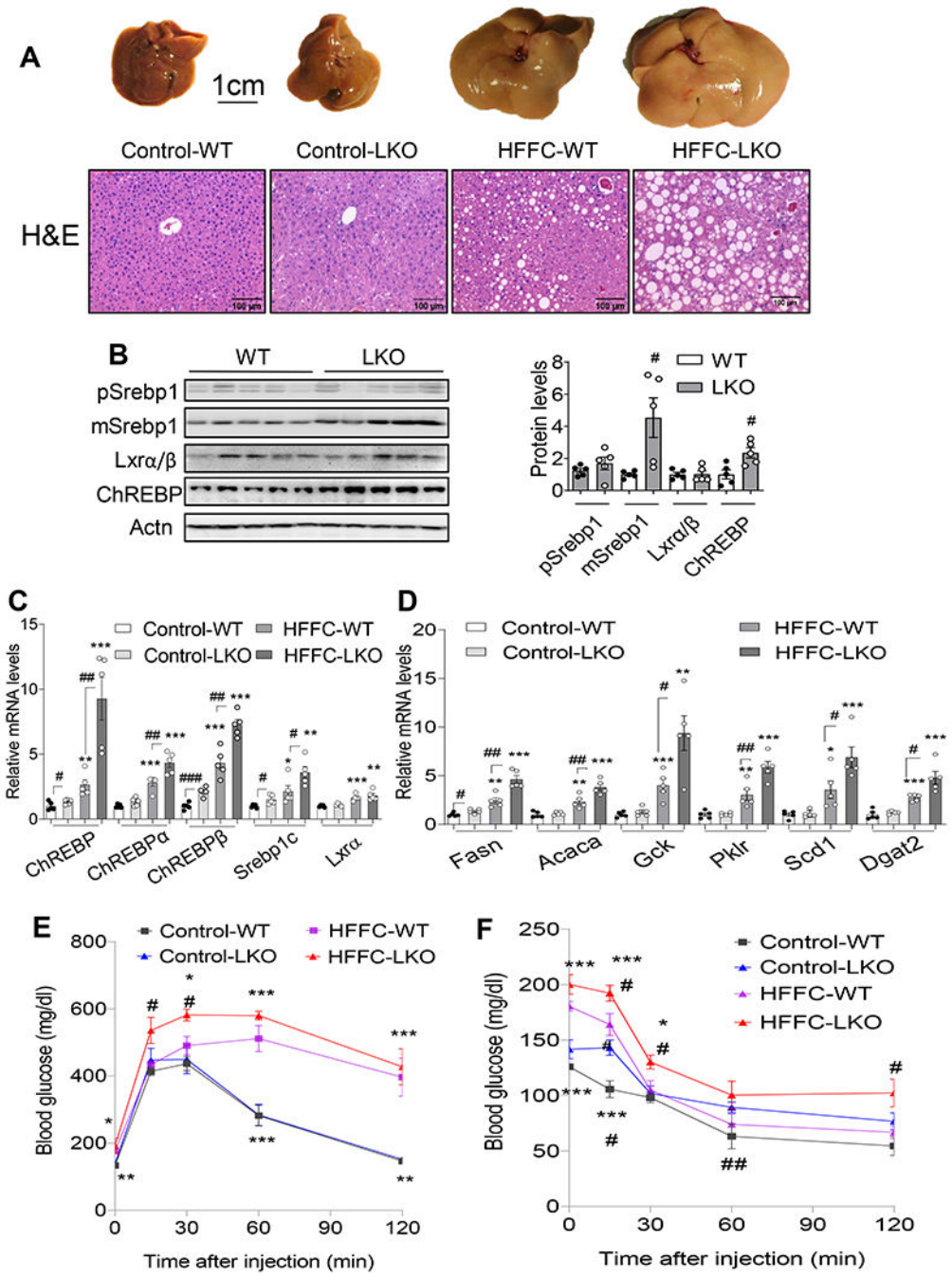

Figure 3. Glucose and lipid metabolism genes are dysregulated in the liver of Sirt6 LKO mice on a HFFC diet.

(A) Gross images of livers and H&E staining of liver sections of WT and Sirt6-LKO male mice fed with the control or HFFC diet for 11 weeks. (B) Western blot and quantification analysis of pSrebp1, mSrebp1, Lxrα/β, and ChREBP in the livers of WT and Sirt6-LKO male mice fed with HFFC diet for 11 weeks (n=5). (C) Real-time PCR analysis of *Chrebp, Srebp1c*, and *Lxrα* in the livers of WT and Sirt6-LKO male mice fed with the control or HFFC diet for 11 weeks (n=5). (D) Real-time PCR analysis of glucose and lipid metabolism genes including *Fasn, Srebp1c, Acaca, Gck, Pklr, Scd1*, and *Dgat2* in the livers of WT and

Sirt6-LKO male mice fed with the control or HFFC diet for 11 weeks (n=5). (E and F) Glucose and insulin tolerance tests in the control or HFFC fed WT and Sirt6-LKO male mice for 10 and 11 weeks, respectively (n=5). Data are presented as mean ± SEM. *P < 0.05, **P < 0.01 and ***P < 0.001 for HFFC vs. control diet for the same genotype; #P < 0.05, and ##P < 0.01 for LKO vs. WT in the same diet.

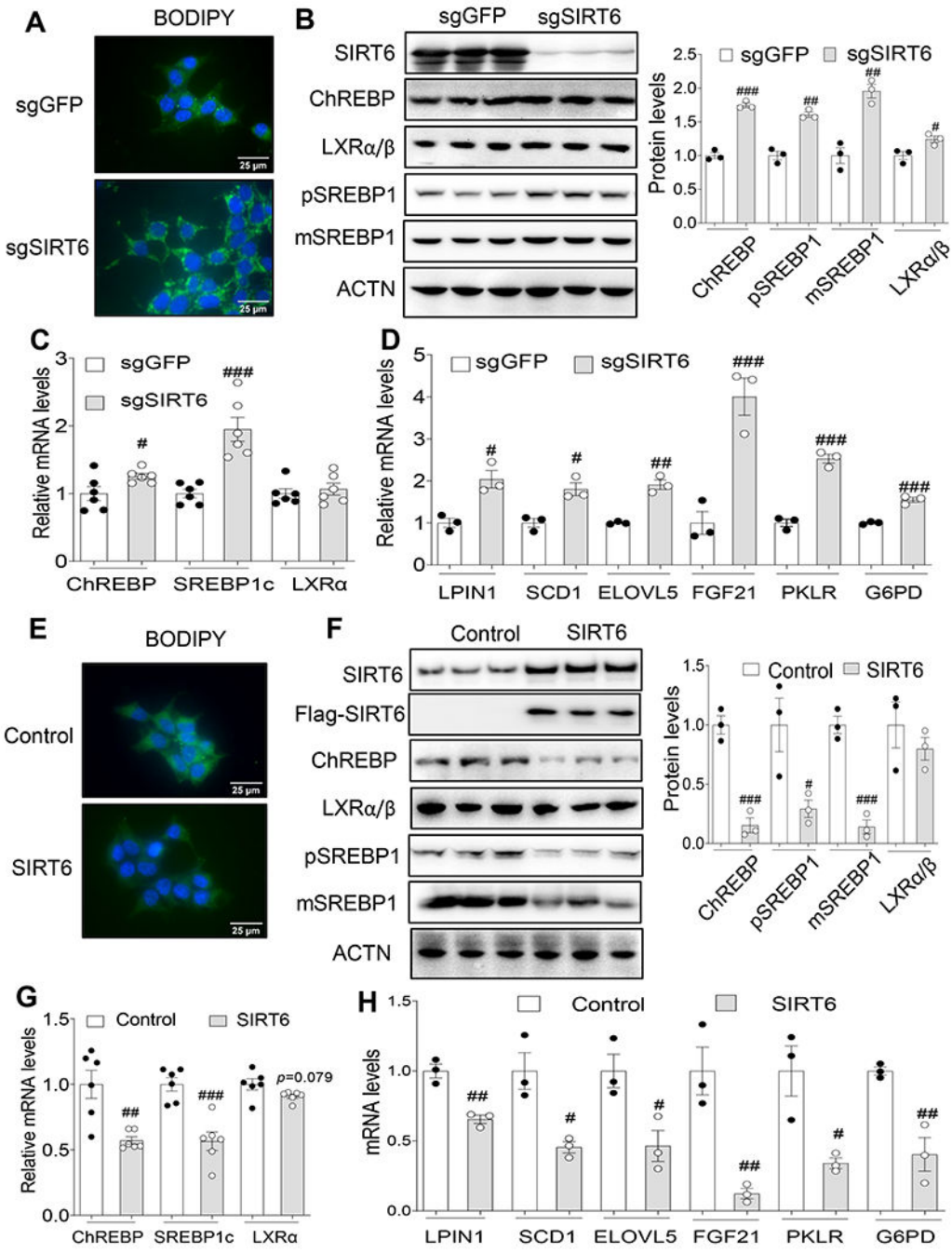

Figure 4. SIRT6 suppresses hepatic lipogenesis through downregulation of key lipogenic regulators.

(A) BODIPY staining of neutral lipids in Huh7 cells that were transfected with control sgGFP or sgSIRT6 CRISPR-Cas9 plasmids. (B) Western blot and quantification analysis of SIRT6, ChREBP, LXRα/β, pSREBP1, and mSREBP1 proteins in the Huh7 cells transfected with control sgGFP or sgSIRT6 plasmids (n=3). (C) Real-time PCR analysis of *ChREBP, SREBP1c*, and *LXRα* mRNAs in the Huh7 cells transfected with control sgGFP or sgSIRT6 plasmids (n=6). (D) Real-time PCR analysis of *LPIN1, SCD1, ELOVL5, FGF21, PKLR*, and *G6PD* mRNAs in Huh7 cells transfected with control sgGFP or sgSIRT6 plasmids

(n=3). (E) BODIPY staining of neutral lipids in Huh7 cells that were transfected with control vector or SIRT6 overexpression plasmids. (F) Western blot and quantification analysis of SIRT6, ChREBP, LXRα/β, pSREBP1, and mSREBP1 proteins in the Huh7 cells transfected with control vector or SIRT6 overexpression plasmids (n=3). (G) Real-time PCR analysis of *ChREBP, SREBP1c*, and *LXRα* mRNAs in the Huh7 cells transfected with control vector or SIRT6 overexpression plasmids (n=6). (H) Real-time PCR analysis of *LPIN1, SCD1, ELOVL5, FGF21, PKLR*, and *G6PD* mRNAs in the Huh7 cells transfected with control vector or SIRT6 overexpression plasmids (n=3). Data are presented as mean ± SEM. #p < 0.05, and ##p < 0.01, and ###p < 0.001 vs. control.

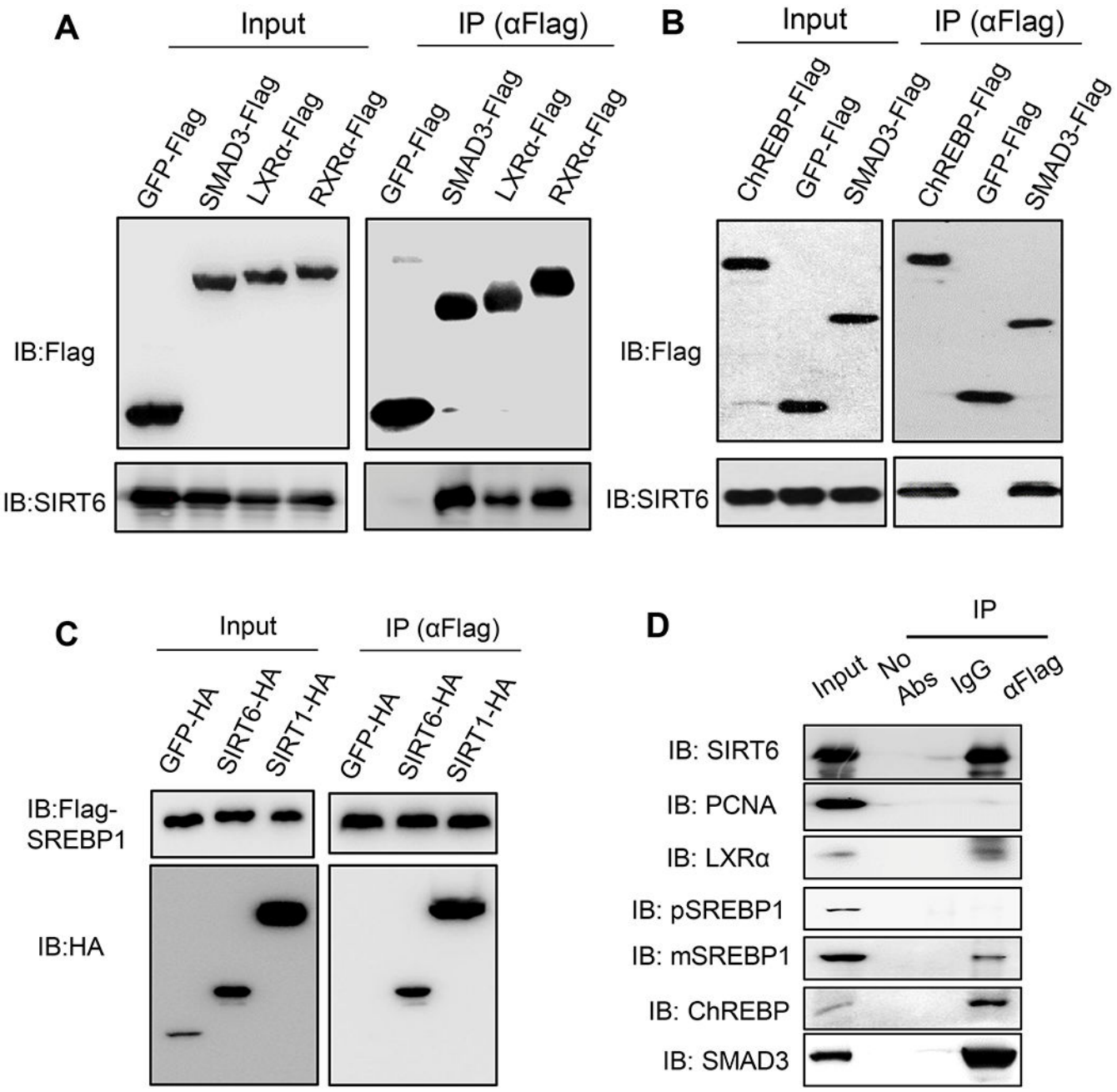

Figure 5. SIRT6 interacts with key lipogenic regulators.

(A) Co-immunoprecipitation (IP) analysis of interactions between SIRT6 and LXRα or RXRα in Huh7 cells. SMAD3 was used here as a positive control. (B) Co-IP analysis of an interaction between SIRT6 and ChREBP in Huh7 cells. (C) Co-IP analysis of an interaction between SIRT6 and SREBP1c in Huh7 cells. (D) Co-IP analysis of interactions between Flag-Sirt6 and endogenous LXRα, SREBP1c, and ChREBP in Huh7 cells.

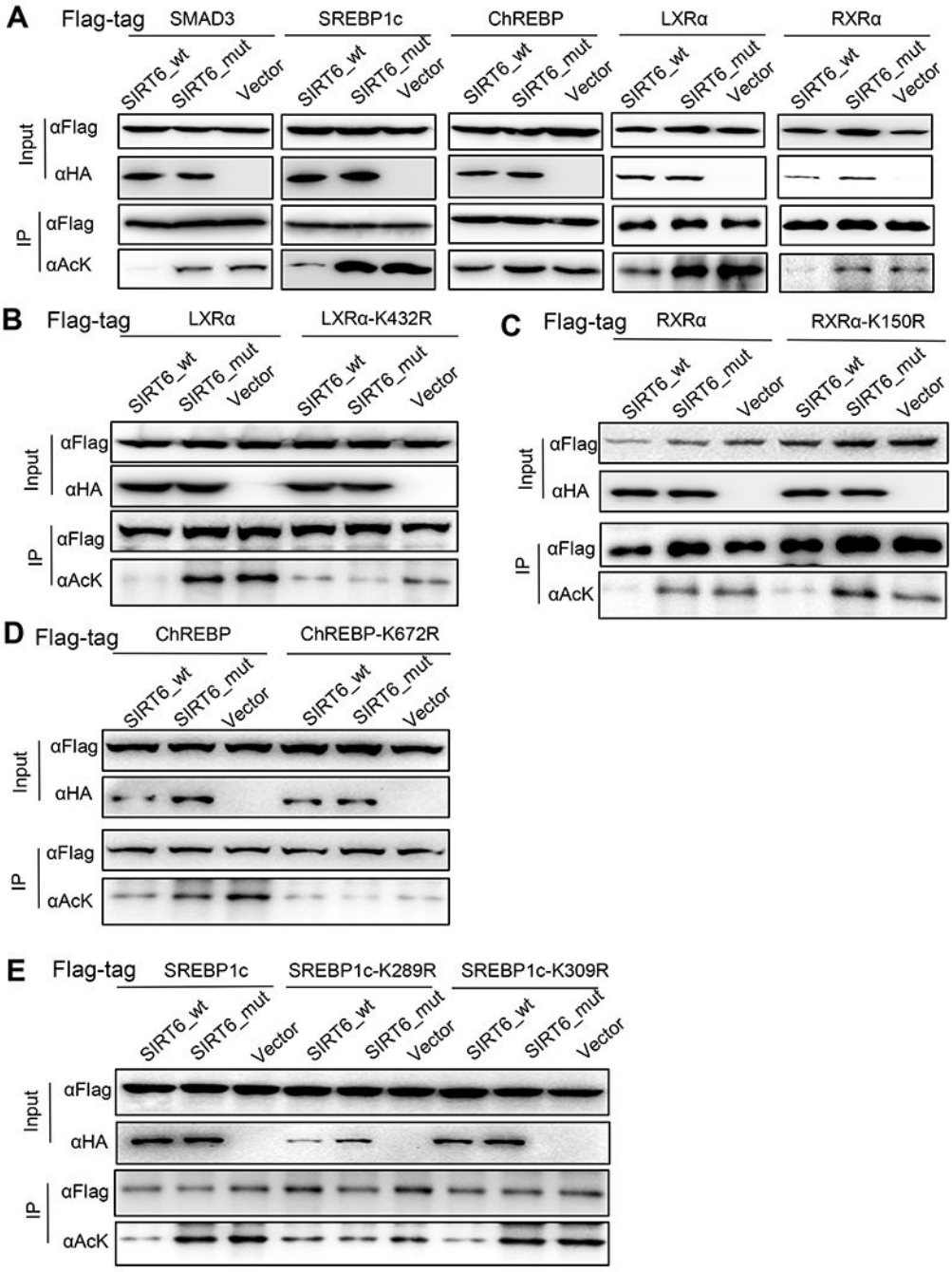

Figure 6. SIRT6 deacetylates key lipogenic regulators.

(A) SMAD3, SREBP1c, ChREBP, LXRα, and RXRα acetylation analysis in Huh7 cells transfected with SIRT6_wt, SIRT6_H133Y mutant (mut), or vector control plasmids. SMAD3 was used here as a positive control. (B) Western blot analysis of deacetylation of WT and mutant LXRα (K432R) by WT or mutant SIRT6. (C) Western blot analysis of deacetylation of WT and mutant RXRα (K150R) by WT or mutant SIRT6. (D) Western blot analysis of deacetylation of WT and mutant ChREBP (K672R) by WT or mutant SIRT6. (E)

Western blot analysis of deacetylation of WT and mutant SREBP1c (K289R and K309R) by WT or mutant SIRT6.

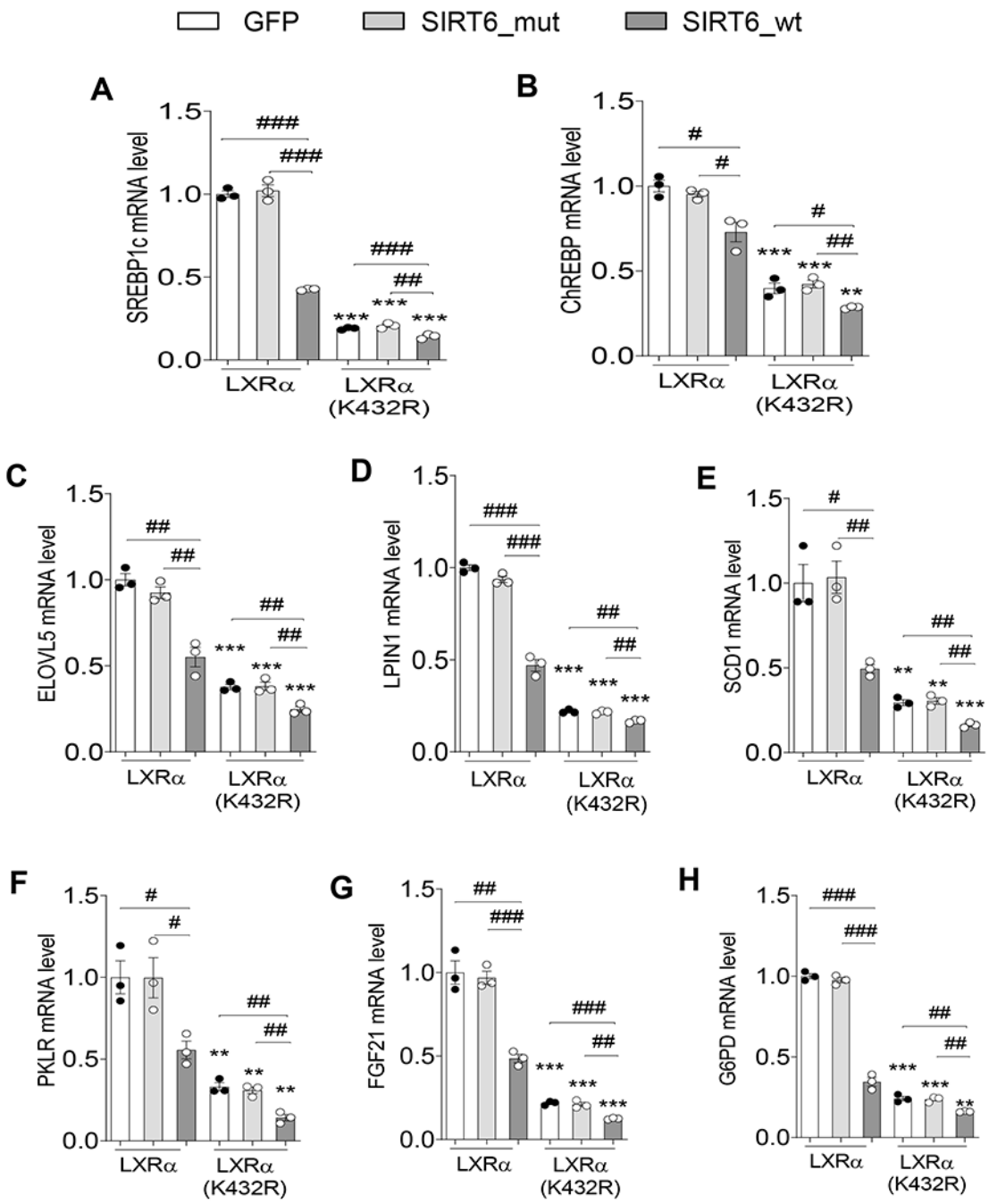

Figure 7. SIRT6 attenuates the LXRα transcriptional activity via deacetylation.

(A-H) Real-time PCR analysis of the effect of LXRα deacetylation by SIRT6 on metabolic gene expression in Huh7 cells. Data are presented as mean ± SEM. n=3. **p < 0.01 and ***p < 0.001 for mutant LXRα vs. WT LXRα under the same treatment; #p < 0.05, ##p < 0.01, and ###p < 0.001.

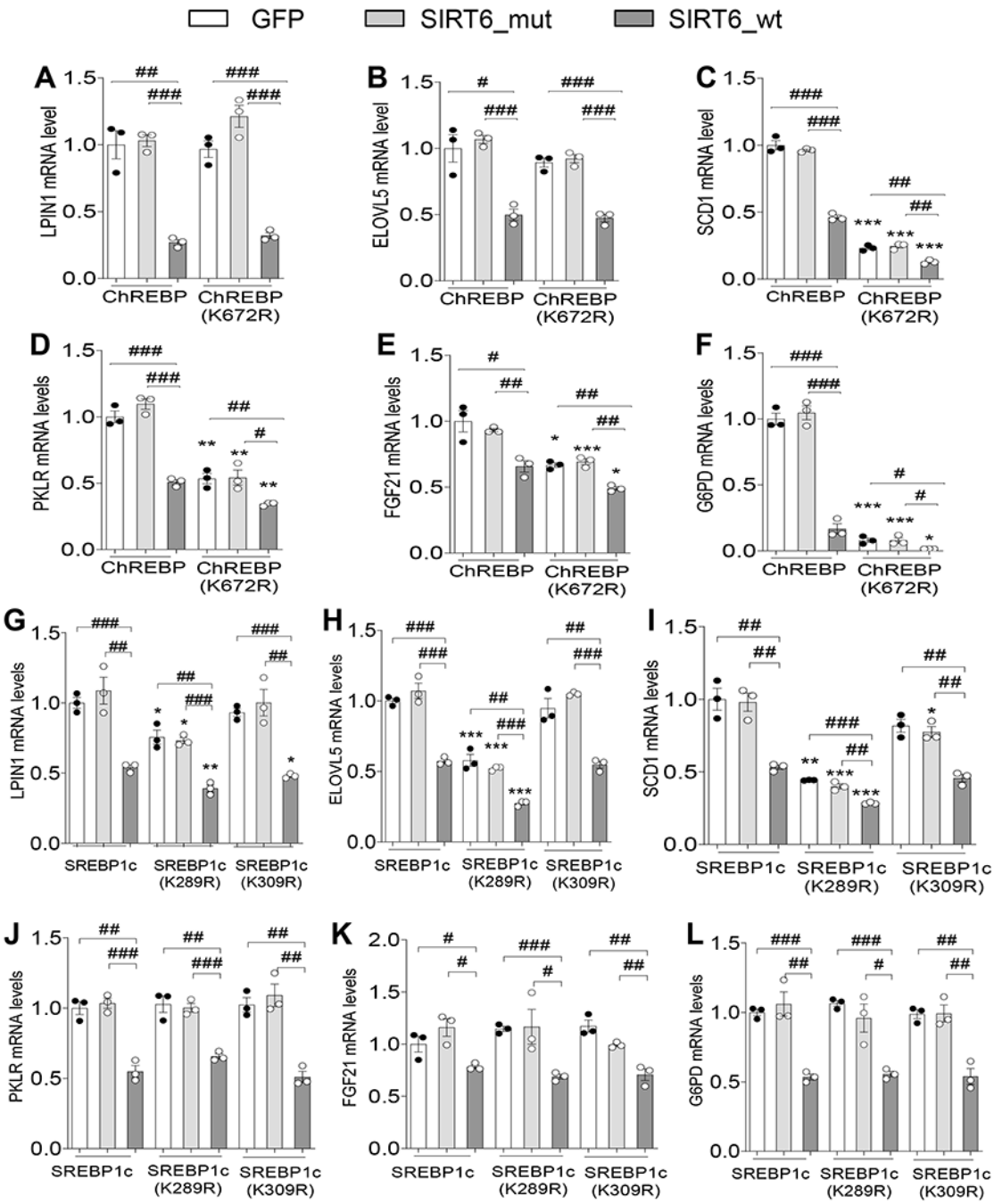

Figure 8. SIRT6 attenuates the transcriptional activity of ChREBP and SREBP1c via deacetylation.

(A-F) Real-time PCR analysis of the effect of ChREBP deacetylation by SIRT6 on metabolic gene expression in Huh7 cells. (G-L) Real-time PCR analysis of the effect of SREBP1c deacetylation by SIRT6 on metabolic gene expression in Huh7 cells. Data are presented as mean ± SEM. n=3. *p < 0.05, **p < 0.01 and ***p < 0.001 for mutant ChREBP or SREBP1c vs. WT counterpart under the same treatment; #p < 0.05, ##p < 0.01, and ###p < 0.001.